



HAL
open science

Fatigue residual strength of circular laminate graphite-epoxy composite plates damaged by transverse load

G. Minak, P. Morelli, A. Zucchelli

► **To cite this version:**

G. Minak, P. Morelli, A. Zucchelli. Fatigue residual strength of circular laminate graphite-epoxy composite plates damaged by transverse load. *Composites Science and Technology*, 2009, 69 (9), pp.1358. 10.1016/j.compscitech.2008.05.025 . hal-00537999

HAL Id: hal-00537999

<https://hal.science/hal-00537999>

Submitted on 20 Nov 2010

HAL is a multi-disciplinary open access archive for the deposit and dissemination of scientific research documents, whether they are published or not. The documents may come from teaching and research institutions in France or abroad, or from public or private research centers.

L'archive ouverte pluridisciplinaire **HAL**, est destinée au dépôt et à la diffusion de documents scientifiques de niveau recherche, publiés ou non, émanant des établissements d'enseignement et de recherche français ou étrangers, des laboratoires publics ou privés.

Accepted Manuscript

Fatigue residual strength of circular laminate graphite-epoxy composite plates damaged by transverse load

G. Minak, P. Morelli, A. Zucchelli

PII: S0266-3538(08)00214-5
DOI: [10.1016/j.compscitech.2008.05.025](https://doi.org/10.1016/j.compscitech.2008.05.025)
Reference: CSTE 4092

To appear in: *Composites Science and Technology*

Received Date: 21 December 2007
Revised Date: 16 April 2008
Accepted Date: 26 May 2008

Please cite this article as: Minak, G., Morelli, P., Zucchelli, A., Fatigue residual strength of circular laminate graphite-epoxy composite plates damaged by transverse load, *Composites Science and Technology* (2008), doi: [10.1016/j.compscitech.2008.05.025](https://doi.org/10.1016/j.compscitech.2008.05.025)

This is a PDF file of an unedited manuscript that has been accepted for publication. As a service to our customers we are providing this early version of the manuscript. The manuscript will undergo copyediting, typesetting, and review of the resulting proof before it is published in its final form. Please note that during the production process errors may be discovered which could affect the content, and all legal disclaimers that apply to the journal pertain.



Fatigue residual strength of circular laminate graphite-epoxy composite plates damaged by transverse load

G. Minak*, P. Morelli, A. Zucchelli

*Alma Mater Studiorum - University of Bologna, Department of Mechanical
Engineering (DIEM), Bologna, 40136 v.le Risorgimento 2, Italy*

Abstract

The research dealt with the relation between damage and tension-tension fatigue residual strength (FRS) in a quasi-isotropic carbon fibre reinforced epoxy resin laminate. The work was organized in two phases: during the first one, composite laminates were damaged by means of an out-of-plane quasi-static load that was supposed to simulate a low velocity impact; in the second phase, fatigue tests were performed on damaged and undamaged specimens obtained from the original composite laminates. During the quasi-static transverse loading phase, damage progression was monitored by means of Acoustic Emission (AE) technique. The measurement of the strain energy accumulated in the specimens and of the acoustic energy released by fracture events made it possible to estimate the amount of induced damage and evaluate the quasi-static residual tensile strength of the specimens. A probabilistic failure analysis of the fatigue data, reduced by the relative residual strength values, made it possible to relate the FRS of damaged specimens with the fatigue strength of undamaged ones.

Key words: A. Carbon fibre, B. Fatigue, B. Impact behaviour, C. Probabilistic methods, D. Acoustic emissions

1 Introduction

The use of carbon fibre reinforced plastics (CFRP) in the transport industry (mainly airborne, but also naval and automotive) is spreading because of their

* Corresponding author.

Email addresses: giangiaco.minak@unibo.it (G. Minak),
piero.morelli@unibo.it (P. Morelli), a.zucchelli@unibo.it (A. Zucchelli).

high specific strength and stiffness that allow great weight savings over metallic materials. Durability and damage tolerance are two important issues that in the past limited the application of CFRP to particular fields such as sports competitions or luxury products, where the peak performances, rather than safety and availability, are the main objectives.

However, this class of materials can be degraded due to accidental loads, such as low energy and velocity impacts [1-4]. An analysis of probable impact events on an airplane is described by Hosur et al. [5]. Symons and Davis [6] report that most of the studies focus on the investigation of quasi-static compression resistance after impact, and fatigue resistance in tension-compression or in compression-compression. The principal failure mechanism in these cases is the progressive delamination near the damaged zone and the consequent reduction of the critical buckling load. They conclude also that residual tensile strength and tension-tension fatigue strength of impact damaged composite laminates are relatively affected.

Nevertheless, there are cases in which the stress status is mainly tensile (e.g. in vessels subject to internal pressure). In [7], Cesari et al. found a significant reduction of the static tensile strength in quasi-isotropic CFRP specimens with visible damage due to transverse load.

In the present study the tension-tension ($\sigma_{min}/\sigma_{max} = 0.01$) fatigue behaviour of plain and damaged composite laminas was studied. Damage was induced by quasi-static transverse loads that were supposed to simulate low velocity impacts [8-13]. The Acoustic Emission technique [14-18] was used, during the quasi-static transverse loading tests, in order to monitor the material damage progress and to measure the intensity of the emitted acoustic energy, which is required by the method proposed in [17], for the estimation of the quasi-static residual ultimate tensile strength (σ_{U^*}) of the laminates.

Concerning the AE physics, when components are loaded stress redistributions can occur, due to irreversible phenomena caused by damage mechanisms. Part of the elastic strain energy is therefore released in the form of heat and elastic waves, which can be detected at the surface of the material by means of piezoelectric devices and transduced into electrical signals, called AE signals. Among the available AE analysis techniques [18], the AE signal features approach was used to identify the locations of AE sources and measure the amplitude, duration and energy of AE events. Damage monitoring was based on the definition of a “sentry” function taking into account the strain energy (E_s), which is related to the integrity of the material, and the AE events energy (E_a), which is rather related to the damage intensity. The definition of the “sentry” function as $f = \ln(E_s/E_a)$ has proven to be a useful indicator of the damage progression during low velocity impact testing [7,17]. Moreover, it was found that the integral \mathcal{J}_f of the sentry function over the indenter displacement is related with the quasi-static residual ultimate tensile strength of

the material [17].

2 Material and Methods

Composite square $250 \times 250 \times 1.6$ mm graphite/epoxy laminate plates, the same studied in [7,17], were tested. The laminates were made in an autoclave from pre-pregs by stacking eight unidirectional plies in the quasi-isotropic $[0/90/+45/-45]_s$ lay-up. In order to induce controlled damage in the material, specimens were placed in a circular clamping fixture, with an internal diameter of 200 mm, and they were loaded at the centre [7]. The indentation tool was a hardened steel sphere with a radius of 7 mm. Transverse load was applied by means of a servo-hydraulic Instron 8033 testing machine controlled by a MTS Teststar II system and equipped with a 25 kN load cell. The specimens were loaded monotonically in control of displacement with a speed of 0.05 mm/s. Each test was stopped at a displacement value chosen among a set of three predetermined levels, roughly corresponding to light, intermediate and severe damage. The actual damage intensity was quantified by the AE method.

AE was monitored by a Physical Acoustic Corporation (PAC) PCI-DSP4 device with four PAC R15 transducers placed around the indentation area, as shown in Fig. 1. This setup allowed the localization and evaluation of the damaged zone extension. After each quasi-static transverse loading test, the damaged plate was sliced by a diamond saw, either in the parallel direction to the external ply fibers, or in the perpendicular direction, as shown in Fig. 1, where the white dots represent the AE source locations. The cuts were performed in order to keep the damaged zone at the centre of the fatigue specimens.

The fatigue residual strength of the composite laminate was investigated as a function of the two stacking sequences ($[0/90/+45/-45]_s$ and $[90/0/+45/-45]_s$). The tensile specimens had the same geometry suggested by ASTM D 5766 for open hole testing of CFRP, with a width of 40 mm and a length of 250 mm. Analogous tensile tests were run on plain specimens cut from undamaged zones of the same plates. Fatigue tests were performed by means of an Instron 8032 servo hydraulic machine equipped with a FastTrack 8800 digital electronic in load control with a frequency of 5 Hz.

2.1 Life data model

The fatigue failure probability of specimens was modeled [19] as a function of the applied stress (normalized with respect to the ultimate tensile strength) and the resulting life, on the basis of the following two hypotheses:

- a) fatigue life, as the number of cycles N , is a Weibull distributed stochastic variable, whose failure probability density function is:

$$f(N, \alpha, \beta) = \frac{\beta}{\alpha} \left(\frac{N}{\alpha}\right)^{\beta-1} e^{-\left(\frac{N}{\alpha}\right)^\beta} \quad (1)$$

where α is the characteristic life and β the shape parameter of the distribution;

- b) the characteristic life α is in a typical power relation with the intensity of the normalized stress σ [20]:

$$\ln(\alpha) = \gamma_1 + \gamma_2 \cdot \sigma \quad (2)$$

Under these assumptions, the failure probability distribution expressed in Eq. 1 is a function of the applied stress, the fatigue life and three parameters of the model:

$$f = f(N, \sigma; \beta, \gamma_1, \gamma_2) \quad (3)$$

The values of the parameters β , γ_1 and γ_2 can be determined by a Maximum Likelihood Estimate performed on the experimental data. In the logarithmic form, the likelihood function \mathcal{L} is as follows:

$$\mathcal{L}(\beta, \gamma_1, \gamma_2) = \sum_{i=1}^k \mathcal{L}_i + \sum_{j=1}^h \mathcal{L}_j \quad (4)$$

where \mathcal{L}_i is the i^{th} log-likelihood contribution of the k data set of failed specimens:

$$\mathcal{L}_i(\beta, \gamma_1, \gamma_2) = \ln [f(N_i, \sigma_i; \beta, \gamma_1, \gamma_2)] \quad (5)$$

and \mathcal{L}_j is the j^{th} log-likelihood contribution of the h censored data set of run out specimens:

$$\mathcal{L}_j(\beta, \gamma_1, \gamma_2) = \ln \left[1 - \int_0^{N_j} f(t, \sigma_j; \beta, \gamma_1, \gamma_2) dt \right] \quad (6)$$

The optimum values of the parameters $(\beta, \gamma_1, \gamma_2)$, that allow the model to provide the best interpolation of the experimental measures, are found by maximizing the log-likelihood function.

2.2 Statistical data analysis

In order to draw a comparison on the effects of the different test conditions on specimen fatigue properties, the *Likelihood Ratio Method* [19,20] was used. This method provides a test for the comparability of several data populations, that have been processed using the same statistical model. The likelihood ratio method requires the calculation of maximum log-likelihood values for each data set and for the pooled data, in order to define the T statistics as follows:

$$T = 2 \left| \sum_{i=1}^{N_{sets}} \mathcal{L}_i - \mathcal{L}_P \right| \quad (7)$$

where N_{sets} is the number of different data sets to be considered in the comparison, \mathcal{L}_i is the maximum log-likelihood value for the i^{th} data set and \mathcal{L}_P is the maximum log-likelihood value for the pooled data.

The T statistics are then compared to the chi-square distribution $\chi^2(1 - \delta, G)$, where $(1 - \delta)$ is a suitable confidence level and G is the number of degrees of freedom of the probability distribution function used in the model (for the case of Eq. 1, $G = 3$).

If $T \leq \chi^2(1 - \delta, G)$, it is possible to conclude, at the selected confidence level, that the specimen groups belong to the same population.

In the opposite case, at least one data set and its related failure probability model, show a statistically significant difference in respect to the pooled data, and it is possible to conclude that the specimens belong to different populations.

2.3 Sentry function

In order to study the damage originated in the laminates by transverse indentation, the “sentry” function $f(x) = \ln[E_s(x)/E_a(x)]$ proposed in [17] was applied. The function $f(x)$ is defined over the discontinuous Ω_{AE} part of the indenter displacement domain, where the acoustic energy E_a is non zero. Depending on the severity of the impact-like testing, the resulting $f(x)$ can assume any combination of the four $P_i(x)$ behaviours shown in Fig. 2. In particular, the increasing $P_I(x)$ trend is due to an increasing deformation of the plate with the accumulation of strain energy E_s without noticeable damage progression, while the sudden drops described by $P_{II}(x)$ like functions reveal high E_a energy related with severe damage events. The constant and the decreasing behaviours shown by $P_{III}(x)$ and $P_{IV}(x)$ types of functions are related to high AE activity that overcomes the strain energy storing capability of the material. This is an indication for incipient failures.

In order to quantify the overall amount of damage induced in the laminates, the integral \mathcal{J}_f of the function $f(x)$ over the acoustic domain Ω_{AE} was calculated [17]:

$$\mathcal{J}_f = \int_{\Omega_{AE}} \ln \left[\frac{E_s(x)}{E_a(x)} \right] dx \quad (8)$$

The load levels for the execution of the fatigue tests were chosen using a previously determined relation [17] between the values of \mathcal{J}_f measured during the transverse loading phase and the residual ultimate tensile strength σ_{U^*} of the damaged specimens. This relation depends on the orientation of the lamination sequence, with respect to the in-plane tensile loading direction. In particular, for the lay-ups under consideration, the relation found takes the form of Eq. 9 and is plotted in Fig. 3.

$$\sigma_{U^*} = A \cdot e^{-\left(\frac{\mathcal{J}_f}{B}\right)^C} \quad (9)$$

The numerical values of the parameters A , B and C are listed in Table 1. The values were calculated by implementing a best fit of Eq. 9 on the experimental measures of the quasi-static tensile residual strength obtained in [17].

3 Results and Discussion

3.1 Transverse loading tests

Table 2 shows the values of the maximum load (L_{max}), maximum displacement (D_{max}) and \mathcal{J}_f for each tested lamina. L_{max} was measured by a 25 kN Instron load cell, while D_{max} was measured by the Linear Variable Differential Transformer (LVDT) displacement transducer of the testing machine. The values of \mathcal{J}_f for the tested conditions were between 104.8 mm and 152.9 mm. The ratio between \mathcal{J}_f and D_{max} was calculated, giving out a mean value of 18.0 and a standard deviation of 1.8, which is an indication of a roughly linear proportionality between the damage quantifier \mathcal{J}_f and the transverse displacement of the plate along the centerline of the point of indentation. The regularity of the \mathcal{J}_f/D_{max} ratio is an indication for the comparability of the laminate behaviours during the impact-like damaging phase of the plates.

3.2 Fatigue tests

Pulsating tensile fatigue loading was applied with a load factor $\sigma_{min}/\sigma_{max} = 0.01$ at room temperature. Different failure mechanisms were observed for plain and damaged specimens and within damaged ones between short-life (failed before 10^4 cycles) and long-life (failed after 10^5 cycles) specimens. In the $[90/0/+45/-45]_s$ plain specimens, failure started with matrix cracking (clearly visible to the naked eye). An extensive delamination started from the free edges in the $0^\circ/45^\circ$ interfaces and finally the 45° and 0° fibres broke. In the $[0/90/+45/-45]_s$ plain specimens, failure began with an extensive delamination starting from the free edges in the $90^\circ/45^\circ$ interfaces and finally the 90° and 0° fibres broke.

As far as damaged specimens are concerned, few differences were found in failure mechanics of the two stacking sequences. The ones subject to loads higher than 80% the ultimate residual tensile strength σ_{U^*} , were characterized by matrix cracking of the 90° plies, for the case of $[90/0/+45/-45]_s$ specimens, and longitudinal splitting on the face that was previously quasi-statically indented (front face \mathcal{F}), while the other face (rear face \mathcal{R}) was affected by the propagation of cracks in the direction perpendicular to the specimen axis.

Specimens loaded at stress levels lower than 80% σ_{U^*} , on the contrary, showed the propagation of an elliptic shaped delamination on the \mathcal{R} face, from the beginning of fatigue testing. The ellipse originated around the damaged zone and was oriented at a 45° angle with respect to the specimen axis. Later on, during the progression of fatigue testing, longitudinal splitting appeared on the \mathcal{F} face.

Fatigue life diagrams of the two lay-ups are shown in Figs. 4 and 5. Stress intensities are expressed as percentages of the ultimate tensile strength σ_{uts} of plain (undamaged) specimens [7]. The experimental points are drawn together with the 10%, 50% and 90% iso-failure probability curves, as calculated according to the Weibull model of Eq. 1, whose parameters are listed in the left side of Table 3 for each of the four data sets.

As expected, damaged specimens were characterized by a lower fatigue strength. A comparison between fatigue behaviour of the two stacking sequences outlines the better performances observed for the $[90/0/+45/-45]_s$ lay-up, even though, in this case, data are slightly more dispersed.

Fatigue diagrams depend on both the specimen lay-up and the amount of damage accumulated during the preliminary transverse indentation phase.

In order to assess the fatigue behaviour of the material as an exclusive function of the lay-up, it was necessary to reduce the intensity of the applied fatigue stress with regard to the estimated residual ultimate tensile strength σ_{U^*} of each specimen. The modified fatigue data are plotted in Fig. 6, where the i^{th}

load level is expressed as a percentage of the i^{th} specimen σ_{U^*} , as calculated by Eq. 9. The parameters of the probabilistic failure model for the fatigue data aggregated in this form are given in Table 3, as a function of the two lay-up varieties.

A T-test was carried out on the modified fatigue data, calculating the T statistics as provided in Eq. 7. The right side of Table 3 shows the maximum log-likelihood values $\mathcal{L}_{\vartheta,1 \rightarrow 2}$ of the four σ_{U^*} normalized data sets, and the maximum log-likelihood values $\mathcal{L}_{\vartheta,P}$ for the σ_{U^*} normalized pooled data. Eq. 7 gives:

$$T_{0^\circ} = 2 \cdot |\mathcal{L}_{0^\circ,1} + \mathcal{L}_{0^\circ,2} - \mathcal{L}_{0^\circ,P}| = 3.2$$

$$T_{90^\circ} = 2 \cdot |\mathcal{L}_{90^\circ,1} + \mathcal{L}_{90^\circ,2} - \mathcal{L}_{90^\circ,P}| = 5.6$$

Taking into consideration a confidence level of $(1-\delta) = 95\%$, for $G = 3$ degrees of freedom of the model, the χ^2 function assumes the value of $\chi^2(0.95, 3) = 7.81$, which is greater than T_{0° and T_{90° .

Within a confidence level of at least 95%, it is therefore possible to conclude that both the reduced data sets of plain and damaged specimens belong to the same population, and can be treated as homogeneous data.

4 Conclusions

The FRS of damaged CFRP laminates was investigated and compared with the fatigue strength of the undamaged material. For the case of pre-damaged specimens, during the quasi-static transverse indentation loading phase, the Acoustic Emission technique was applied and the integral measure \mathcal{J}_f of the ratio between two energy parameters was used, in order to quantify the amount of damage induced in the laminates.

A first probabilistic failure analysis was performed on the experimental data, providing a classic model for the fatigue behaviour of the material, as a function of the lay-up and the initial damage. A relation between the \mathcal{J}_f damage parameter and the expected residual ultimate tensile strength σ_{U^*} of each specimen was then used in order to arrange fatigue data in a form that is influenced by the lay-up direction only. As a result, a second probabilistic failure analysis of the reduced fatigue data proved that it is possible to evaluate the FRS, at the desired reliability extent, using the fatigue life curve of the undamaged material, once the applied load has been reduced with the σ_{U^*} value derived from the initial damage amount.

A statistical analysis of the reduced data showed significant differences be-

tween the fatigue behaviour of $[0/90/+45/-45]_s$ and $[90/0/+45/-45]_s$ stacking sequences, the latter providing better strength performances. Assuming that the failure model was independent of the initial damage amount, as previously specified, it is possible to conclude that the direct exposure at the specimen surface of 0° plies (layers of the most importance, since their fibre orientation is parallel to the loading direction) weakens the component, with respect to the laminate's ideal durability, due to the wider fatigue fracture vulnerability of external plies.

5 Acknowledgements

The authors thank Dr. Daniele Ghelli for his precious help in setting up the experimental tests, and the Italian Ministry of University and Research for funding this study.

References

- [1] Abrate S. Impact on laminated composite materials. *Appl Mech Reviews* 1991;44(4):155-190.
- [2] Abrate S. Impact on laminated composites: recent advances. *Appl Mech Reviews* 1994;47(11):517-544.
- [3] Abrate S. Impact on composite structures. Cambridge University Press, 1998.
- [4] Cantwell WJ, Morton J. The impact resistance of composite materials, a review. *Composites* 1991;22(5):347-362.
- [5] Hosur MV, Murty CRL, Ramamurthy TS, Shet A. Estimation of impact-induced damage of CFRP laminates through ultrasonic imaging. *NDT&E Intl* 1998;31(5):359-374.
- [6] Symons DD, Davis G. Fatigue testing of impact-damage T300/914 carbon-fibre-reinforced plastic. *Comp Sci Tech* 2000;60(3):379-389.
- [7] Cesari F, Dal Re V, Minak G, Zucchelli A. Damage and residual strength of laminated carbon-epoxy composite circular plates loaded at the centre. *Compos Part A* 2007;38(4):1163-1173.
- [8] Caprino G, Langella A, Lopresto V. Prediction of first failure energy of circular carbon fiber reinforced plastic plates loaded at the centre. *Compos Part A* 2003;34:349-357.
- [9] Caprino G, Langella A, Lopresto V. Elastic behaviour of circular composite plates transversely loaded at the centre. *Compos Part A* 2002;33:1191-1197.

- [10] Found MS, Holden GJ, Swamy RN. Static indentation and impact behaviour of GRP pultruded sections. *Compos Struct* 1997;39:223-228.
- [11] Lee SM, Zahuta P. Instrumented impact and static indentation of composites. *J Compos Mater* 1991;25(2):204-220.
- [12] Kwon YS, Sankar BV. Indentation-flexure and low-velocity impact damage in graphite epoxy laminates. *J Compos Tech Res* 1993;15(2):101-111.
- [13] Wardle BL, Lagace PA. On the use of quasi-static testing to assess impact damage resistance of composite shell structures. *Mech Compos Mater St* 1998; 5(1):103-121.
- [14] Benmedakhene S, Kenane M, Benzeggagh ML. Initiation and growth of delamination in glass/epoxy composites subjected to static and dynamic loading by acoustic emission monitoring. *Comp Sci Tech* 1999;59:201-208.
- [15] Siron O, Tsuda H. Acoustic emission in carbon fibre-reinforced plastic material. *Ann Chim Sci Mat* 2000;25(7):533-537.
- [16] Scott G, Scala CM. A review of non-destructive testing of composite materials. *NDT&E Int* 1982;15(2):75-86.
- [17] Minak G, Zucchelli A. Damage evaluation and residual strength prediction of CFRP laminates by means of acoustic emission techniques. *Comp Mat Res Progress*, Nova Science Publishers 2008:167-209.
- [18] Prosser W H. Acoustic Emission, Chapter 6 in *Non-destructive Evaluation, Theory, Techniques and Applications*. P. J. Shull & M. Dekker Inc. editions 2002.
- [19] Nelson W. *Applied life data analysis*. New York: Wiley 1982.
- [20] Goglio L, Rossetto M. Comparison of fatigue data using the maximum likelihood method. *Eng Frac Mech* 2004;71:725-736.

Lay-up	A [MPa]	B [mm ⁻¹]	C
[0/90/+45/-45] _s	610	148.5	2.8
[90/0/+45/-45] _s	610	106.6	2.0

Table 1

Parameters of the $\mathcal{J}_f \leftrightarrow \sigma_{U^*}$ relation.

Specimen	D_{max} [mm]	L_{max} [kN]	\mathcal{J}_f [mm]	\mathcal{J}_f/D_{max}
1	8.5	2.5	140.6	16.5
2	8.2	2.5	146.2	17.8
3	8.1	2.6	137.4	17.0
4	8.8	2.6	145.7	16.6
5	8.3	2.5	134.0	16.1
6	9.1	2.9	151.5	16.7
7	8.4	2.6	131.2	15.6
8	7.0	2.5	132.7	19.0
9	7.6	2.7	146.7	19.3
10	5.7	2.5	128.7	22.6
11	7.6	2.6	142.0	18.7
12	8.6	3.0	152.9	17.8
13	6.9	2.5	135.8	19.7
14	5.8	2.5	104.8	18.1

Table 2

Quasi-static transverse loading test results.

Experimental data set	σ_{uts} normalized data			σ_{U^*} normalized data			
	β	γ_1	γ_2	β	γ_1	γ_2	\mathcal{L}
$[0/90/+45/-45]_s$ Plain	1.95	25.6	-0.224	1.95	25.6	-0.224	$\mathcal{L}_{0^\circ,1} = -74.2$
$[0/90/+45/-45]_s$ Damaged	2.32	21.4	-0.242	2.20	22.8	-0.178	$\mathcal{L}_{0^\circ,2} = -80.2$
$[0/90/+45/-45]_s$ Pooled				1.81	24.6	-0.207	$\mathcal{L}_{0^\circ,P} = -156$
$[90/0/+45/-45]_s$ Plain	1.58	33.5	-0.294	1.58	33.5	-0.294	$\mathcal{L}_{90^\circ,1} = -73.7$
$[90/0/+45/-45]_s$ Damaged	1.24	124	-2.21	1.00	48.6	-0.475	$\mathcal{L}_{90^\circ,2} = -46.5$
$[90/0/+45/-45]_s$ Pooled				1.04	41.0	-0.388	$\mathcal{L}_{90^\circ,P} = -123$

Table 3

Parameters of the Weibull failure probability functions. For the case of plain specimens, σ_{uts} is equal to σ_{U^*} , therefore the parameters don't change.

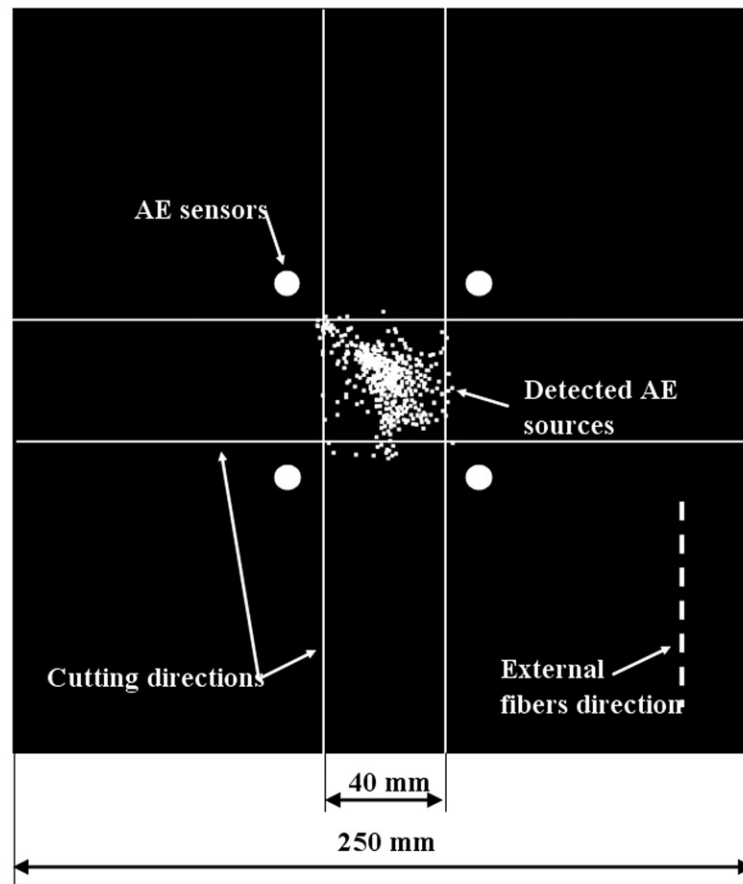


Figure 1. Damaged area detected by AE and cutting directions for fatigue specimens.

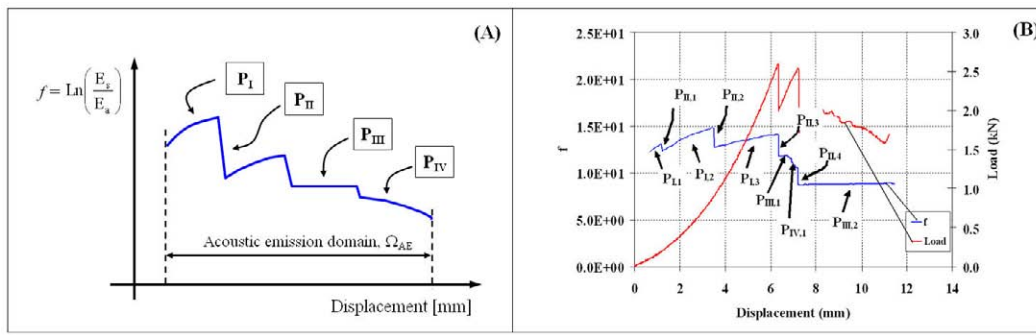


Figure 2. (A) Typical "sentry" function. (B) example of "sentry" function and transverse load vs displacement during an indentation test.

ACCEPTED MANUSCRIPT

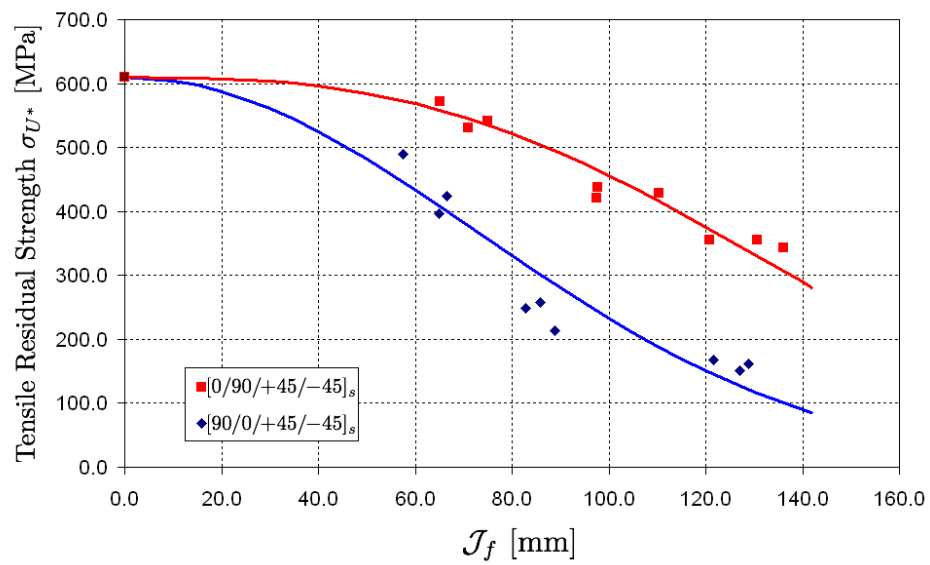


Figure 3. $J_f \leftrightarrow \sigma_{U^*}$ diagrams for the tested lay-ups.

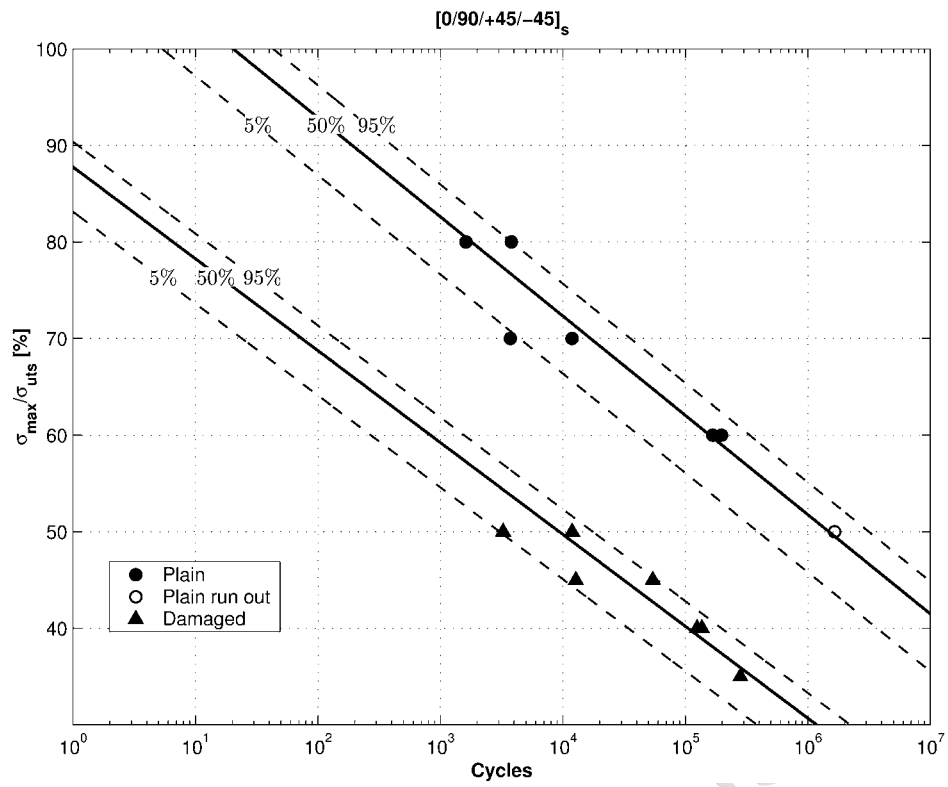


Figure 4. Fatigue diagrams for the $[0/90/+45/-45]_s$ lay-up normalized by σ_{uts} .

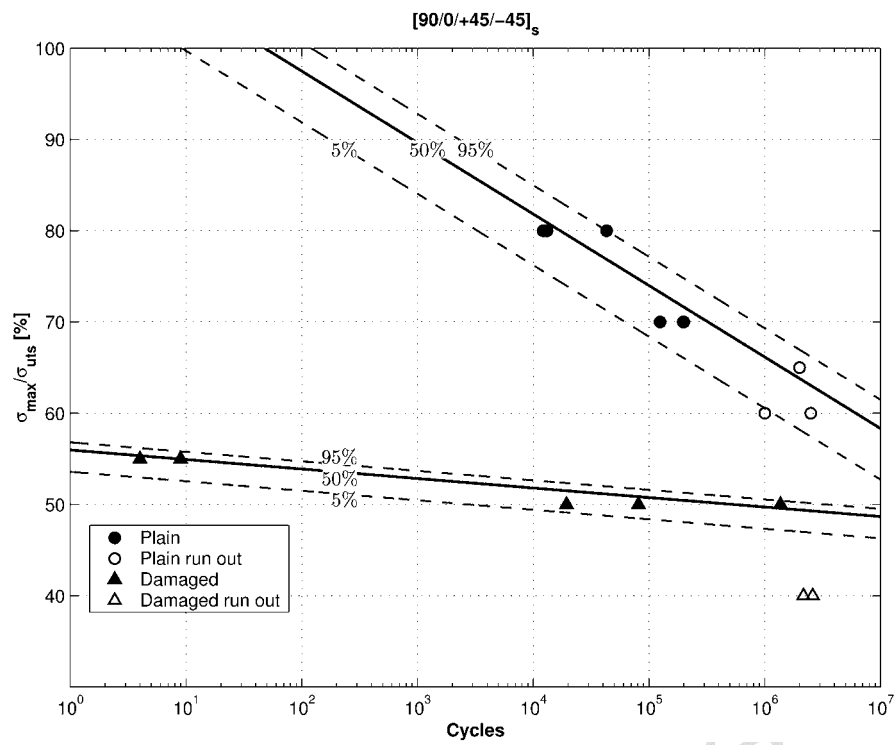


Figure 5. Fatigue diagrams for the [90/0/+45/-45]_s lay-up normalized by σ_{uts} .

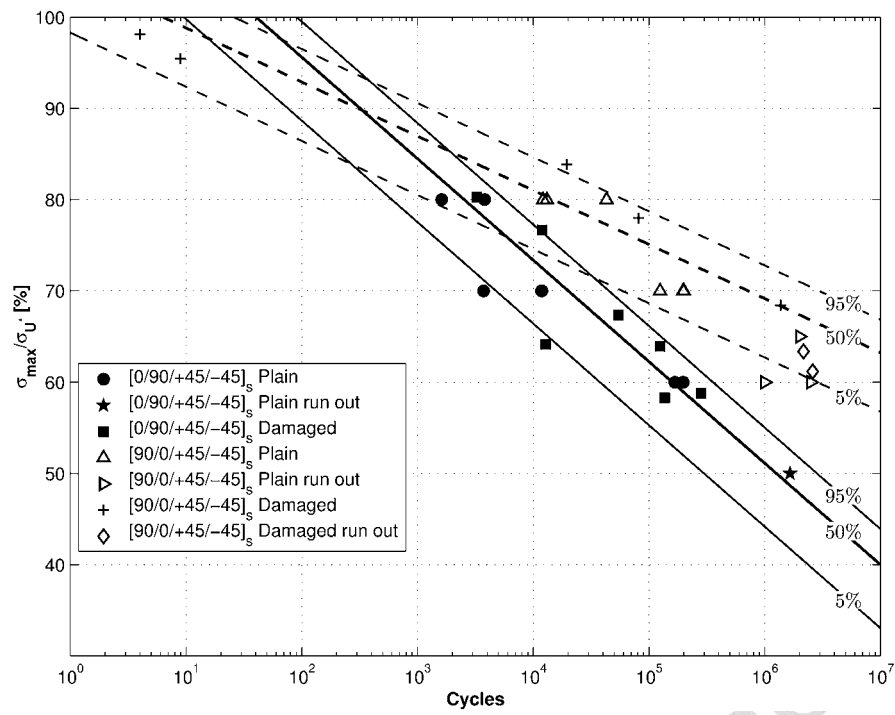


Figure 6. Fatigue diagrams normalized by σ_U^* .

6 Table captions

Table 1. Parameters of the $\mathcal{J}_f \leftrightarrow \sigma_{U^*}$ relation.

Table 2. Quasi-static transverse loading test results.

Table 3. Parameters of the Weibull failure probability functions. For the case of plain specimens, σ_{uts} is equal to σ_{U^*} , therefore the parameters don't change.

7 Figure captions

Figure 1. Damaged area detected by AE and cutting directions for fatigue specimens.

Figure 2. (A) Typical “sentry” function. (B) example of “sentry” function and transverse load vs displacement during an indentation test.

Figure 3. $\mathcal{J}_f \leftrightarrow \sigma_{U^*}$ diagrams for the tested lay-ups.

Figure 4. Fatigue diagrams for the $[0/90/+45/-45]_s$ lay-up normalized by σ_{uts} .

Figure 5. Fatigue diagrams for the $[90/0/+45/-45]_s$ lay-up normalized by σ_{uts} .

Figure 6. Fatigue diagrams normalized by σ_{U^*} .